Bulletin of the JSME Vol.18, No.2, 2024
Journal of Advanced Mechanical Design, Systems, and Manufacturing

Design of micromachines under uncertainty with the sample-average approximation method

Jorge Mario MONSALVE GUARACAO*, Sergiu LANGA*, Michael STOLZ*,
Andreas MROSK*, Bert KAISER* and Harald SCHENK**
* Fraunhofer IPMS, Maria-Reiche-Str. 2, Dresden 01109, Germany
E-mail: jorge.mario.monsalve.guaracao@ipms.fraunhofer.de
** Chair of Micro and Nano Systems, Brandenburg University of Technology Cottbus-Senftenberg
Platz der Deutschen Einheit 1, Cottbus 03046, Germany

Received: 23 November 2023; Revised: 6 January 2024; Accepted: 24 January 2024

Abstract
Variability in the features produced by microfabrication processes, as well as uncertainty in some material properties, may cause a significant deviation in the performance of micromachines within the same fabrication run. Based on an estimation of the expected process variations, the design of such devices can be optimised to achieve the design goals, even under this uncertainty. Learning from previous works on the design of microresonators, we formulate this design problem as a case of chance-constrained optimisation and expand it to a general case where both the dynamic sensitivity ought to be maximised and the natural frequency should be close to a given target. Constraints to ensure a safe operation under both static and dynamic conditions are included by means of penalty functions. We implement the 'Sample-Average Approximation' (SAA), known in the field of stochastic programming, to solve the problem with a single-objective genetic algorithm (CMA-ES), requiring only a numerical evaluation of the objective function—no computation of its gradient is required nor a specific analytic form. We apply this optimisation strategy to the design case of an ultrasonic transducer—'lateral CMUT'—, using optical measurements of trench variability to estimate process variations in a hypothetical design. Comparison of different optimisation results reveals that the implementation of SAA enables the choice of a more conservative design that meets the targets in spite of variability in its features.

Keywords : Robust design, Parameter uncertainty, Micro Electro-Mechanical Systems (MEMS), Stochastic programming, Covariance Matrix Adaptation – Evolution Strategy (CMA-ES)

1. Introduction

Whereas the development of precision machining has enabled the fabrication of components in the millimetre range with tolerances in the micrometre range (Dornfeld and Lee, 2010), certain processes in micromachining still yield variations in the sub-micrometre range for components in the micrometre range. For instance, Deep Reactive-Ion Etching (DRIE), a common bulk micromachining process that offers great flexibility to carve trenches of arbitrary shapes, is known to produce non-uniform features, both depending on the feature size and its position in the wafer, because of the complex physical and chemical processes that are involved (Díaz, 2010). In some cases, not only are devices fabricated with variable dimensions but also the material properties may fluctuate depending on the fabrication process (see, for example, the analysis of Sharpe et al. (2001) on the Young's Modulus of polycrystalline silicon). Under these conditions, a design with deterministic assumptions becomes unsatisfactory, for, though the 'ideal' device might achieve the targeted performance, it might not be found in the actual fabrication run. The statistical nature of microfabrication calls, therefore, for a statistical approach in the design of micromachines, where the expected variations are estimated a priori and an optimization strategy is contrived in such a way that the design targets are met in spite of the expected variations.

Paper No.23-00540
[DOI: 10.1299/jamdsm.2024jamdsm0018]

© 2024 The Japan Society of Mechanical Engineers. This is an open access article under the terms of the Creative Commons Attribution-NonCommercial-NoDerivs license (https://creativecommons.org/licenses/by-nc-nd/4.0/).

Some previous works on the topic of MEMS[1] design under uncertainty present interesting strategies applied to the case of resonators (Fan et al., 2005; Hsiung, 2006; Mawardi and Pitchumani, 2005). A common tenet in these works is that the expected value of the objective function ought to be optimised, instead of its nominal value. From the beginning, it is assumed that the design parameters are governed by random distributions and thus the objective function will be described by a random distribution as well. In the case of a resonator, the objective function is the square of the difference between the actual and targeted natural frequency. Fan et al. (2005) performed a first-order Taylor expansion of the objective function and observed that this expected value can be expressed as the sum of a deterministic component (depending only on nominal values) and a random component (depending on the variance of the parameters). In order to apply their method, the gradient of the objective function with respect to each parameter must be known (together the expected variance of each parameter). With this approach, an initially single-objective, deterministic optimisation problem is turned into a multi-objective, stochastic one, where the deterministic and random components represent conflicting goals. A similar multi-objective optimisation was proposed by Safaie et al. (2014) for the design of an electro-thermal actuator, in which case the variable of interest is the static deflection. They postulated the problem as the conflicting maximisation of the actuator's nominal deflection and the minimisation of its variance. Alternatively, they suggested that a single-objective optimisation could be performed if the actuator's deflection is set as a constraint and its variance is minimised.

The design of micromachines, nonetheless, need not focus merely on targeting a resonance frequency or maximising the static sensitivity, but may combine both aspects and include further considerations. This is the case of electroacoustic transducers and accelerometers, where both the sensitivity ought to be maximised and the resonance frequency should lie either within a specific margin or above a certain value, depending on the application. In addition, the safe operation of the device under both static and dynamic loading must be ensured. Saghir et al. (2021) consider these multiple variables in the design of a MEMS accelerometer and formulate a multi-objective optimisation, simultaneously seeking (among others) for a maximum sensitivity, a maximum voltage for static failure, and a minimum resonance frequency—not yet considering process variability. We depart from this multi-objective approach towards a single-objective one, where one clear goal is prioritised for maximisation and the other design considerations (such as target resonance and safe operation) are formulated as constraints. Furthermore, we argue that the stochastic problem of maximising an expected value need not be split into a multi-objective problem with a deterministic and a random component, but it can be solved as a single-objective problem by means of the Sample-Average Approximation, a technique well known in the field of stochastic programming (Kim et al., 2015; Wang et al., 2022). In this work, we implement a widespread generic algorithm known as CMA-ES[2] (Hansen and Ostermeier, 1996; Nagata, 2004) to find the global maximum of the objective function. The use of CMA-ES is advantageous as it does not require any knowledge of the gradient of the objective function nor any specific analytic formulation (such as the posynomials proposed by Hsiung (2006)), but it can be directly coupled to a numerical model, even a finite-element simulation script (Schuffenhauer, 2017). This article is based on the results of a previous conference presentation of ours (Monsalve et al., 2023) and expounds with more rigor a methodology that can be applied to micromachines in general, not only ultrasonic transducers.

2. Formulation of the optimisation problem

The CMA-ES algorithm is suited to find the global maximum of a multivariate function whose arguments are bounded between 0 and 10, that is,

$$\begin{aligned} &\text{Maximise: } f(\vec{x}) \\ &\text{Subject to:} \\ &0 \leq x_i \leq 10 \quad i = 1, \dots, N \end{aligned} \tag{1}$$

This is achieved by generating random 'mutations' of the parameters and using the information of the 'fittest' parameter sets to generate the next 'offspring'; therefore, it finds the 'fittest' parameter set after a certain amount of 'generations'

[1] Micro Electro-Mechanical Systems

[2] Covariance Matrix Adaptation – Evolution Strategy

[DOI: 10.1299/jamdsm.2024jamdsm0018]
© 2024 The Japan Society of Mechanical Engineers

by mimicking natural selection. No knowledge of the gradient of the function is required, only its evaluation. If the design problem can be formulated in the form of Eq. (1), its solution can be effectively found with CMA-ES.

The first task in the formulation of the design problem is the choice of the objective function. Let the variable to be maximised be the amplitude of the transducer's linearised transfer function at the frequency of operation ($|H(\omega_c)|$). This scalar variable can be further split into a static sensitivity (H_0) times a dynamic factor, which depends on the working frequency (ω_c), the natural frequency (ω_n) and the Q factor ($f_{dyn}(\omega_c, \omega_n, Q)$). It is common in MEMS design to cram multiple, nearly identical oscillators onto a given chip area, in which case their amount (N_{osc}) multiplies the sensitivity as well—notice how the calculation of N_{osc}, an integer number, introduces step-like discontinuities in the objective function. All these variables that comprise the target function ought to be expressed in terms of a vector variable containing all the design parameters, $\vec{p}_{nom}$.

Having formulated an objective function, the restrictions for optimisation can be defined. A straightforward set of restrictions follows from the limitations of the fabrication process, which set lower and upper bounds on each of the design parameters ($p_{nom,i}$). Regarding the natural frequency, instead of minimising the error with respect to a target value (thus having two conflicting design goals), one can set the constraint that this frequency be within a tolerable interval, thereby defining 'prohibited regions' in the search space. (If, however, the application is stricter on the natural frequency than on the sensitivity, the former can be formulated as the target, and it can be required that the latter be no less than a certain acceptable value.) An additional set of restrictions originates from the requirements for safe operation, both static and dynamic. Broadly speaking, the static load (e.g. the dc voltage) at which failure occurs (P_{cr}) must be higher than a certain safety limit imposed by the designer (P_{safe}), and the Q factor ought not to be higher than a certain limit (Q_{safe}) in order to avoid dynamic failure. Even if a particular design problem is not well described by these restrictions, these three cases are a good illustration of different sorts of restrictions: a tolerance range, a maximum acceptable value, and a minimum acceptable value.

Following the elegant formulation of Hsiung (2006), the latter considerations can be expressed as a chance-constrained optimisation problem in the following manner ($\boldsymbol{E}\{\}$ being an expected value and $\boldsymbol{P}\{\}$ being a probability):

$$
\begin{aligned}
&\text{Maximise:} \quad f(\vec{p}_{nom}) = \boldsymbol{E}\{N_{osc} H_0 f_{dyn}(\omega_c, \omega_n, Q)\} \\
&\text{Subject to:} \\
&\boldsymbol{P}\{(\omega_n(\vec{p}_{nom}) - \omega_c)^2 > \delta_\omega^2\} \leq \epsilon \\
&\boldsymbol{P}\{P_{cr}(\vec{p}_{nom}) < P_{safe}\} \leq \epsilon \\
&\boldsymbol{P}\{Q(\vec{p}_{nom}) > Q_{safe}\} \leq \epsilon \\
&p_{min,i} \leq p_{nom,i} \leq p_{max,i} \quad i = 1, \ldots, N
\end{aligned}
\tag{2}
$$

Notice that the random variables from which the associated probabilities arise are not explicitly defined in Eq. (2). The rationale is that each set of nominal parameters, $\vec{p}_{nom}$, is associated with a random process that results in a distribution of values of H_0, ω_n, P_{cr}, etc—the particular model for such a distribution is left open for the designer. By maximising the expected value, the overall performance of the fabrication run is optimised, as opposite to the performance of an ideal single device. The stochastic formulation of the constraints requires, not that the respective limits never be violated, but that the probability of such an event taking place be limited to a very small value (ϵ).

[DOI: 10.1299/jamdsm.2024jamdsm0018]
© 2024 The Japan Society of Mechanical Engineers

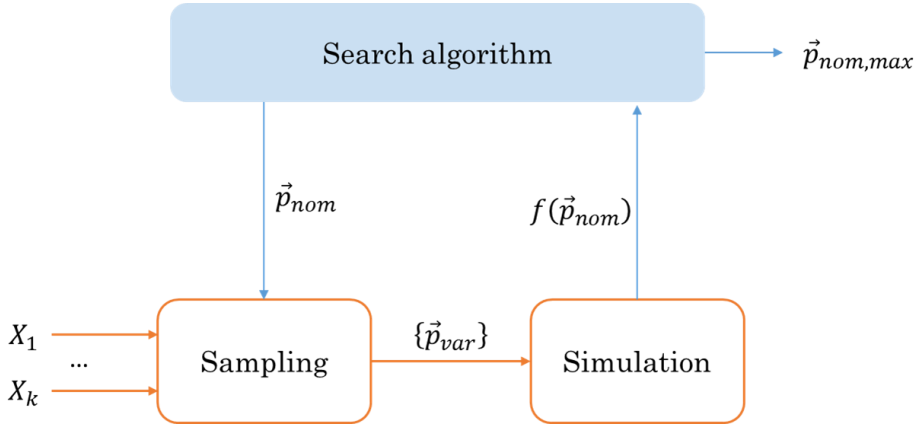

Fig. 1 Scheme of a procedure for optimisation based on Sample-Average Approximation (SAA). A multivariate search algorithm proposes a certain combination of nominal parameters. This combination is then subject to a Monte-Carlo simulation governed by a number of random variables in order to mimic the effect of process variations. With this set of altered parameter combinations, the average of the target function is passed on to the search algorithm so that it seeks for a better combination until an optimal vector of parameters is found.

The Sample-Average Approximation (SAA), as its name indicates, approximates the expected value as the arithmetic mean of a finite number of randomly generated samples (N_{SAA}). This requires that, for each vector of nominal parameters, $\vec{p}_{nom}$, a set of altered parameters, $\{\vec{p}_{var}\}$, suffering the effect of process variations, be generated with the aid of random variables $\{X_k\}$. If a material property is to be varied, then the random samples would not differ in their nominal dimensions but in their performance as they are simulated. In the simplest case, one single random variable would govern the deviation of all parameters, but this need not be the case. There could be multiple independent random variables, and there could be dependent random variables, according to the nature of the stochastic process. What matters to the algorithm is that a representative number of samples be generated, such that the evaluation of the target function and the constraints is precise enough to guide the search of the optimal parameters. This process is illustrated in Fig. 1.

Whilst SAA helps formulating the stochastic problem in (2) in a way that resembles the deterministic problem in (1), the constrains for the natural frequency and safe operation do not fit into the category of a simple upper and lower bound. However, the search algorithm can be made to avoid the prohibited regions in the search space by introducing penalty functions. In an analogue way to natural selection, the randomly generated parameter combinations, $\{\vec{p}_{var}\}$, for which the restrictions are violated, can be punished with a nullified objective function, which will effectively lead the evolutionary strategy away from the undesired parameter sets (as long as the objective function does not change its sign within the search space). We propose the following smooth, exponential functions as penalty functions:

$$\begin{aligned} &\text{Maximise:} \quad f(\vec{p}) = \frac{1}{N_{SAA}} \sum_{\vec{p} \in \{\vec{p}_{var}\}} N_{osc} H_0 f_{dyn} \Pi_U \Pi_Q \Pi_\omega \\ &\text{Subject to:} \\ &p_{min,i} \leq p_{nom,i} \leq p_{max,i} \quad i = 1, \dots, N \end{aligned} \tag{3}$$

Whereby

$$\Pi_U = 1/[1 + \exp(-(U_{PI} - U_{safe})/\epsilon_U)] \tag{4.1}$$

$$\Pi_Q = 1/[1 + \exp((Q - Q_{safe})/\epsilon_Q)] \tag{4.2}$$

$$\Pi_\omega = \exp[-((\omega_n - \omega_c)/\epsilon_\omega)^4/2] \tag{4.3}$$

[DOI: 10.1299/jamdsm.2024jamdsm0018]
© 2024 The Japan Society of Mechanical Engineers

The first two penalty functions will supress the objective function if the pull-in voltage lies below the safety limit and if the Q factor exceeds the safe value (notice the sign difference in the exponential function). In principle, a step function could also be suitable, but the smooth and tuneable transition provided by the exponential function is recommendable to aid the evolutionary strategy. The critical reader might be sceptical about the narrow window function (4.3) that punishes designs with a natural frequency away from the target, as this could compromise convergence of the algorithm by prohibiting most of the search space. This can be circumvented by transforming the search space with a convenient formulation of the design variables, such that this restriction is nearly always met. In simple structures such as beams or disks, the unloaded, undamped natural frequency poses a simple restriction between thickness and length (or radius) of the sort $\omega_n \sim t/L^2$. Instead of varying thickness and length freely, one can be made dependent on the other and a correction factor can be used as a design parameter instead of the dependent dimension. For example: $L = \alpha_L\, L_{ref}\, (t/t_{ref})^{1/2} (\omega_{ref}\, /\omega_c)^{1/2}$. Clearly, the simple square-root dependency is only an approximation, but even with deviations caused by nonlinear effects (e.g. softening due to Coulomb force), the introduction of a correction factor enables the evolutionary strategy to adjust the dependent dimension according to the exact, calculated natural frequency.

Further penalty functions could be introduced for more complex design cases. One possibility could be to require that the device's harmonic distortion be maintained below a certain limit. This could be implemented in a similar way as (4.2). However, this manoeuvre of the penalty functions has limitations, as it could make it impossible for the evolution strategy to find non-zero values. If too many of these are involved, it might be best to solve the problem with less constraints and then adjust the bounds of the parameters accordingly in order to refine the search.

With the previous adjustments, the CMA-ES algorithm can be set-up to optimise the design of a micromachine. All that is required is a holistic numerical model of the device that simulates its static and dynamic behaviour, as well as a fully parametrised chip layout. Given that CMA-ES recommends only using variables contained in the range between 0 and 10, a simple scaling operation has to be performed between the randomly generated $\{\vec{x}_i\}$ in each 'generation' and the actual nominal parameters used in the simulation $\{\vec{p}_i\}$. The information of the estimated variance of the random variables is represented by $\vec{\sigma}_p$. Using the notation suggested by Colette et al. (2013), the steps can be summarised in pseudo-code as follows:

Table 1 Pseudo-code algorithm for CMA-ES optimisation with the Sample-Average Approximation.

Optimisation algorithm: *CMA-ES with SAA*

```
While (not convergence):
    {x_i} ← Ask(CMA-ES)
    {p_i} ← Transform_Parameters(p_min, p_max, {x_i})
        {p_i,j} ← Random Generator(σ_p)  for j = 1, …, N_SAA
        {f_i,j} ← Simulate_Device(p_i,j)
        f_avg,i ← (Σ f_i,j)/N_SAA
    CMA-ES ← Tell(CMA-ES, {x_i}, {f_avg,i})
```

3. Case study: Lateral CMUT

3.1 Device concept and model

We now illustrate the application of this optimisation concept with the design of an electromechanical micro-actuator termed 'lateral CMUT[3]' (Monsalve et al., 2022), illustrated in Fig. 2. It consists of a clamped-clamped microbeam that is pulled towards a stator by means of an electrostatic force. As the beam approaches the stator, the fluid in between is squeezed and pushed in the out-of-plane direction. By applying a voltage, $U(t)$, with both a constant and an alternating component, the beam is deflected towards a working point and made to emit ultrasound as it oscillates. The fabrication of this device is heavily dependent on the DRIE process. The design parameters are therefore the beam's dimensions (length, L, thickness, b, width, h) and the constants defining the gap between beam and stator (g_0,σ). Given the flexibility of DRIE, this gap can be carved with a curved shape so that it is narrower at the beam's ends and wider at the beam's midpoint. In other words, $g(x) = g_0\,(1 + \sigma\phi_0(x))$, where σ is a dimensionless constant that modulates the gap according to a normalised bell-shaped function $\phi_0(x)$. Multiple microbeams can be manufactured in a given chip area, and the layout of the chip can be fully parametrised as a function of these variables.

[3] Capacitive Micromachined Ultrasonic Transducer

[DOI: 10.1299/jamdsm.2024jamdsm0018]
© 2024 The Japan Society of Mechanical Engineers

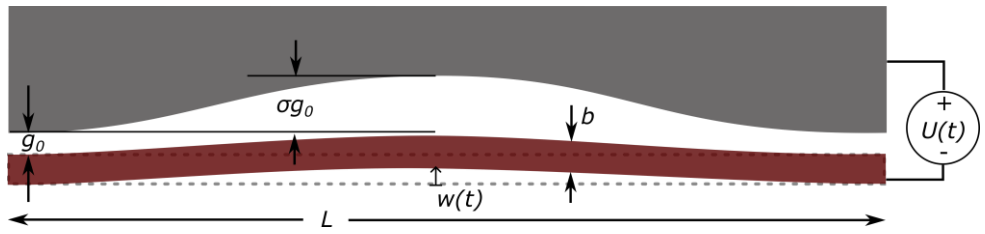

Fig. 2 Scheme of the geometry of a 'lateral CMUT'. A clamped-clamped microbeam (length L, thickness b) is drawn towards a stator by means of an electrostatic force. The gap between the stator and beam need not be of a uniform dimension (g_0) but can be made wider at the midpoint of the beam ($g_0(1+\sigma)$) according to a bell-shaped function.

The optimisation methodology that we present here does not require an analytic model of the device, as long as a numerical simulation can be performed to obtain all the relevant variables (H_0,Q,ω_n,P_{cr}). Nonetheless, given that significant progress has been made to obtain closed-form expressions to describe the behaviour of L-CMUTs, we use the available reduced-order model developed by Schenk et al. (2022) for performing an optimisation. A considerable amount of time is spared if the CMA-ES algorithm, plus the Monte-Carlo simulation involved in SAA, is to be made with closed-form calculations (~ seconds) with respect to a finite-element script (~ hours).

In essence, the reduced-order model of Schenk et al. (2022) is based on the assumption that the deflection profile, both under the static and dynamic loading, is described accurately by the profile of the zeroth oscillation mode, $\psi_0(x) = \cosh(\beta_0 x/L) / \cosh(\beta_0/2) + \cos(\beta_0 x/L) / \cos(\beta_0/2)$. This assumption was validated by both experiments and finite-element simulations. In this work we prefer the notation of the normalised mode, that is, $\phi_0(\xi = x/L) = \psi_0(x/L)/\psi_0(0)$. A consequence of this single-mode approach is that the partial differential equation that governs the beam deflection, $w(x,t)$, is reduced to an ordinary differential equation describing only the deflection at the midpoint $w(0,t)$:

$$m\ddot{w} + c\dot{w} + k_1 w + k_3 w^3 = \frac{C_0}{2g_0}\Gamma_2\left(\frac{w}{g_0} - \sigma\right)U^2(t) - S_p p(t) \tag{5}$$

With $(m,\ c, k_1)$ the lumped mass, damping and stiffness of a typical oscillator, respectively, and k_3 a cubic stiffness proceeding from stress-stiffening. Response to the loads—both voltage (U) and pressure (p)—is characterised by the constants on the right-hand side. The Γ_2 function is given by a power series that can be very well approximated by an algebraic expression:

$$\Gamma_2(x) \approx \frac{1}{77} - \frac{1}{38}(1-x)^{-\frac{1}{2}} + \frac{15}{28}(1-x)^{-\frac{3}{2}} \tag{6}$$

At the biasing point (U_{DC},w_{DC}), the force balance can be linearised as follows:

$$m\ddot{w} + \left(\frac{k_{EM}}{\omega_0 Q}\right)\dot{w} + k_{EM} w = T_{EM} u_{ac} - S_p p(t) \tag{7}$$

Where the following constants have been defined:

$$T_{EM} = \frac{U_{DC} C_0}{g_0}\Gamma_2(z_{DC} - \sigma) \tag{8.1}$$

$$\frac{k_{EM}}{k_1} = 1 + 3\gamma z_{DC}^2 - \frac{(z_{DC} + \gamma z_{DC}^3)\Gamma_3(z_{DC} - \sigma)}{\Gamma_2(z_{DC} - \sigma)} = \frac{\omega_{EM}^2}{\omega_0^2} \tag{8.2}$$

$$\Gamma_3(x) = \Gamma_2'(x) \approx -\frac{1}{162} + \frac{1}{82}(1-x)^{-\frac{1}{2}} - \frac{2}{109}(1-x)^{-\frac{3}{2}} + \frac{62}{77}(1-x)^{-\frac{5}{2}} \tag{8.3}$$

[DOI: 10.1299/jamdsm.2024jamdsm0018]
© 2024 The Japan Society of Mechanical Engineers

(The change of variables $z_{DC} = w_{DC}/g_0$ was introduced for practical purposes.)

The critical static load in electrostatic systems is often the so-called pull-in voltage (U_{PI}), at which the electrodes collapse onto each other due to the nonlinear Coulomb force. The static condition for pull-in is reached when the electromechanical stiffness, k_{EM}, (8.2) reduces to zero, which gives the condition of Eq. (9). Having calculated the critical deflection (z_{PI}, therefore also w_{PI}), the corresponding voltage, U_{PI}, is obtained from Eq. (5).

$$\frac{z_{PI} + \gamma z_{PI}^3}{1 + 3\gamma z_{PI}^2} = \frac{\Gamma_2(z_{PI} - \sigma)}{\Gamma_3(z_{PI} - \sigma)} \approx \frac{64}{97} - \frac{44}{67}(z_{PI} - \sigma) \tag{9}$$

The missing element to perform the optimisation is an estimation of the Q factor. At low enough frequencies, such that $Re = \rho_{air}\,\omega g_0^2/\mu_{air} \ll 1$, the Reynolds equation can be applied to calculate the viscous force acting on the cantilever (Bao and Yang, 2007). Unfortunately, this sets a limit around 10 kHz, depending on the gap size (e.g. 5 µm). Still, usage of the Reynolds equation enabled F. Wall et al. (2023) to obtain an analytic expression for the Q factor of the Coulomb-actuated microbeam, verifying the results against a finite-element model based on the two-dimensional Reynolds equation. Designs at higher frequencies will require an evaluation of the more sophisticated Navier-Stokes equations, either with finite elements or with an analytic simplification. The expression found by Wall et al. (2023) is the following:

$$c_{Re} = \frac{k_{EM}}{\omega_0 Q} = 2\mu_{air} L \left(\frac{h}{g_0}\right)^3 \Gamma_3(z_{DC} - \sigma) \tag{10}$$

An overview of the lumped parameters and their calculation is presented in Table 2.

Table 2 Evaluation of the parameters of the model of Schenk et al. (2022) for a Coulomb-actuated microbeam.

Parameter	Evaluation
Zeroth eigenvalue, β_o	$\tanh(\beta/2) + \tan(\beta/2) = 0$ $\rightarrow \beta_0 \approx 4.730$
Peak of zeroth oscillation eigenmode, ψ_0	$\psi_0 = \frac{1}{\cosh(\beta_0/2)} + \frac{1}{\cos(\beta_0/2)} \approx 1.588$
Integral of the zeroth oscillation eigenmode, χ_1	$\chi_1 = \int_{-\frac{1}{2}}^{\frac{1}{2}} \phi_0(\xi) d\xi \approx 0.5232$
Tensile force integral, χ_3	$\chi_3 = \int_{-\frac{1}{2}}^{\frac{1}{2}} (\phi_0'(\xi))^2 d\xi \approx 4.878$
Duffing coefficient, γ	$\gamma = \left(\frac{6\chi_3\psi_0^2}{\beta_0^4}\right)\frac{g_0^2}{b^2}$
Effective elastic modulus, E'	$E' = \frac{E}{1-\nu^2}$
Linear elastic constant, k_1	$k_1 = \left(\frac{\beta_0^4 E'}{\psi_0^2 L^3}\right)\left(\frac{hb^3}{12}\right)$
Nonlinear elastic constant, k_3	$k_3 = \left(\frac{6\chi_3\psi_0^2}{\beta_0^4}\right)\frac{k_1}{b^2}$
Effective mass, m	$m = \frac{\rho h b L}{\psi_0^2}$
Reference capacitance, C_0	$C_0 = \epsilon_0 \epsilon_r hL/g_0$
Effective acoustic area, S_p	$S_p = \chi_1 hL$
Unbiased natural frequency, ω_0	$\omega_0 = \sqrt{k_1/m}$

[DOI: 10.1299/jamdsm.2024jamdsm0018]
© 2024 The Japan Society of Mechanical Engineers

Resuming the notation of a generic micromachine used in Eq. (2), the static sensitivity, understood as the ratio of displaced air volume per unit ac voltage, is given by $H_0 = S_p T_{EM}/k_{EM}$. (Interestingly, the same expression is obtained for the sensitivity as a microphone, understood as the ratio of displaced charge per unit pressure.) Regarding the dynamic correction factor, f_{dyn}, a first approximation can be made, based on the simple case of a baffled piston, where the frequency response of the radiated pressure is proportional to the piston's acceleration (Beranek, 1993). The acceleration, in turn, is described by the classical response of a second-order, high-pass filter:

$$f_{dyn} = \frac{(\omega_c/\omega_{EM})^2}{\sqrt{(1-\omega_c^2/\omega_{EM}^2)^2 + (\omega_c/(Q\omega_{EM}))^2}} \tag{11}$$

With these expressions, the calculations for a generic MEMS design, as laid out section 2, can be performed: the static sensitivity (H_0), natural frequency (ω_{EM}), Q factor, and critical load (U_{PI}). A staircase function, following from simple geometrical considerations, is further included to calculate the number of beams (N_{osc}) that fit into a given chip area. The capability of CMA-ES to find an optimum design point with such an elaborate objective function involving intricate nonlinear expressions is evidence of its robustness.

3.2 Quantification of process variations

The variation of two characteristic trenches in a fabrication run of an L-CMUT was measured optically in several chips pertaining to the same wafer. It is expected that the wider trench (13 µm by design), without any electrostatic function, exhibit a higher degree of undercut and variance than the narrower trench (5.5 µm by design) that defines the electrostatic gap. A sample microscope picture of these trenches is presented in Fig. 3.

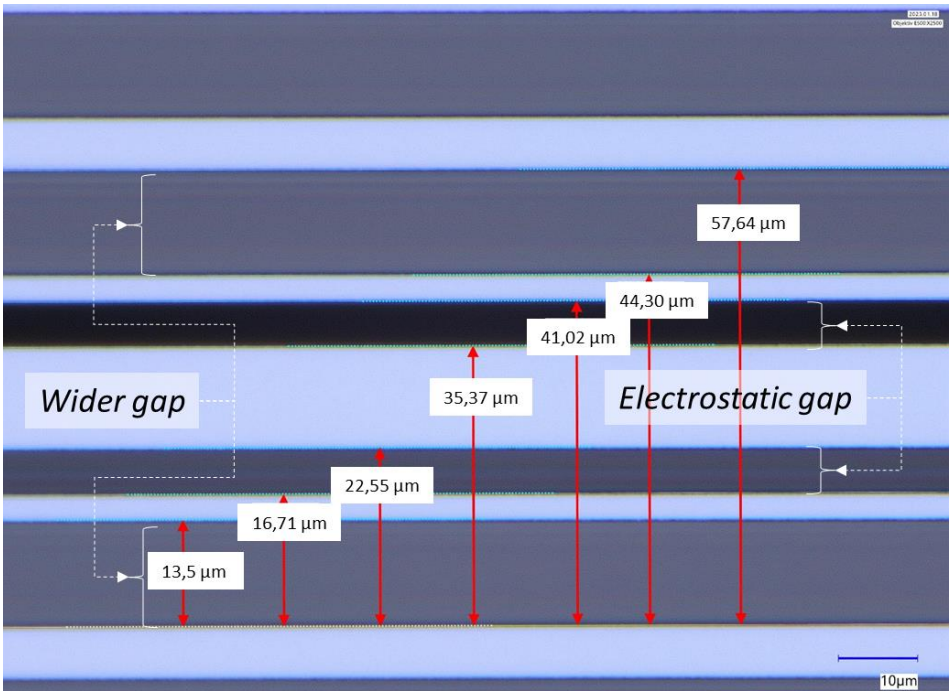

Fig. 3 Sample optical measurement of dimensions in a sample L-CMUT actuator pair (top view). The microbeams are the silicon structures between the trenches termed 'wider gap' and the narrow trenches that define the electrostatic gap. The stator, on the other hand, is the structure between the two consecutive electrostatic gaps.

The measured values, plotted against the radial position of the chip, are shown in Figs. 4 and 5. Given that every feature is measured twice in the same picture, the difference between measurements of the same feature was used to estimate the systematic error due to the manual edge detection, which resulted in 0.1 µm in average. Figures 4 and 5 reveal a tendency for the trenches to become wider near the edge of the wafer, an effect related to the DRIE chamber design. Nonetheless, chips lying in the same radius of the wafer still exhibit a significant degree of variability. A simple

[DOI: 10.1299/jamdsm.2024jamdsm0018]
© 2024 The Japan Society of Mechanical Engineers

standard deviation of the measurements yields 0.17 µm for the wider trench and 0.15 µm for the narrower trench. These values will be used as a first approximation for the expected variance of the respective trenches in a hypothetical design in the upcoming section.

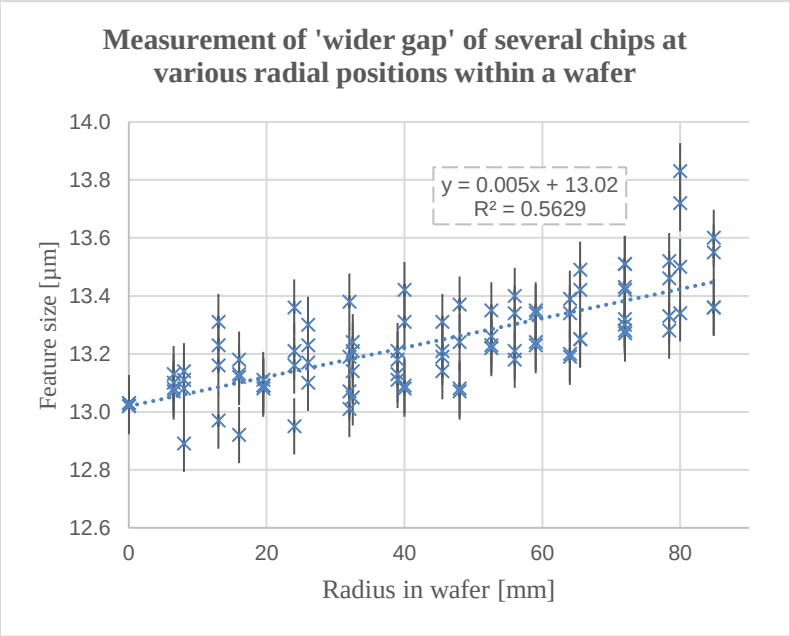

Fig. 4 Plot of the measured ‘wider gap’ as a function of the radial position of the selected chip in the wafer. The uncertainty bars represent the estimation of the optical measurement error.

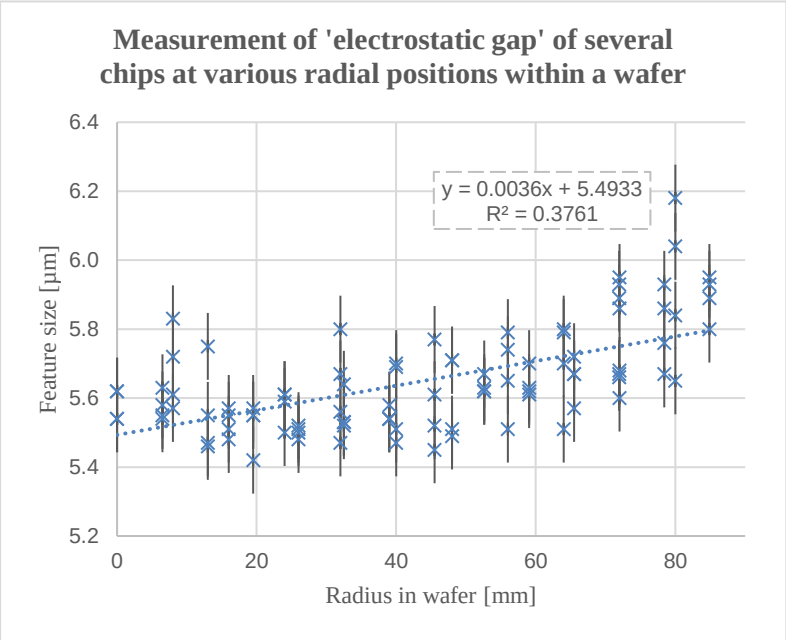

Fig. 5 Plot of the measured electrostatic gap (narrower gap) as a function of the radial position of the selected chip in the wafer. The uncertainty bars represent the estimation of the optical measurement error.

We modelled the variability of DRIE with a single Gaussian process of unit variance ($X \sim N(0,1)$). This assumes that, within the same chip, all the trenches of the narrow type (i.e. those that define the electrostatic gap) will have the same degree of undercut—the lateral etching beneath the lithography mask. However, from chip to chip there will be a deviation from the nominal value that is governed by the aforementioned variable X, which is scaled by 0.15 µm as the measurements reveal. Given that the wider trench has a higher degree of undercut, we assume that this trench is governed by the same Gaussian process but scaling the variable instead by 0.17 µm. This simplification (instead of

[DOI: 10.1299/jamdsm.2024jamdsm0018]
© 2024 The Japan Society of Mechanical Engineers

assuming two independent random processes) is related to the tendency for chips near the wafer edge to exhibit more undercut than chips near the centre, and it reduces the computational cost of the optimisation routine.

4. Application of the optimisation strategy

In order to illustrate the effectiveness of the proposed optimisation strategy, a hypothetical L-CMUT design will be now sought after. Let the targeted operation frequency be 20 kHz with a tolerance margin of ± 5%. We desire the pull-in voltage to be no less than 25 V and the Q factor to be no more than 2. The chip area was limited to a square with a side length of $\lambda/2 \approx 8.5$ mm. Moreover, the parameters were restricted by the following bounds:

$$3\ \mu\text{m} \leq b_{nom} \leq 6\ \mu\text{m} \tag{12.1}$$

$$0.9 \leq \alpha_L \leq 1.2 \tag{12.2}$$

$$2.5\ \mu\text{m} \leq g_{0,nom} \leq 6\ \mu\text{m} \tag{12.3}$$

$$0 \leq \sigma \leq 1 \tag{12.4}$$

The width of the beam is fixed at 75 µm because it is defined by the wafer's thickness.

We compared the following three optimisation cases to appreciate the effect of the dynamic behaviour and the consideration of process variations:

- **Case I:** Deterministic optimisation (no process variations). Dynamic sensitivity is dismissed (Q factor is ignored).
- **Case II:** Deterministic optimisation (no process variations). Dynamic sensitivity is considered (Q factor is calculated).
- **Case III:** Stochastic optimisation with SAA (50 random samples). Dynamic sensitivity is considered (Q factor is calculated).

Case I serves to illustrate the case of a mere electromechanical design without considering acoustic friction losses. One would expect the optimisation routine to converge towards a thin beam and a narrow gap to maximise both the compliance ($1/k_{EM}$) and the transduction coefficient (T_{EM}), as long as the lower limit for pull-in is not trespassed. Case II, on the other hand, should consider the trade-off between Q factor and transduction coefficient and so converge towards a wider electrostatic gap than in Case I. By introducing the Sample-Average Approximation, Case III should serve as a correction for Case II, very likely with a thicker beam, so that the expected process variations cause a lesser impact on the variance of both the sensitivity and the natural frequency.

Table 3 Result of three optimisation cases of an L-CMUT design for operation at 20 kHz.

Variable	Case I	Case II	Case III
Optimised parameters			
b_{nom} [µm]	3.00	3.12	4.20
L_{nom} [µm]	1167	1209	1387
$g_{0,nom}$ [µm]	2.81	5.29	4.65
σ	1.0	1.0	0.98
N_{osc}	1512	1296	1224
Performance metrics (mean ± st. dev.) Monte-Carlo simulation with 256 samples			
H_0 [µm³/mV]	2.99±0.42	0.77±0.14	0.83±0.11
f_{EM} [kHz]	19.7±1.0	19.7±0.99	20.1±0.79
Q	0.25 ±0.02	1.92±0.27	1.73±0.19
U_{PI} [V]	26.8±0.96	99.1±7.1	71.3±4.3
$H_0 f_{dyn} N_{osc}$ [µm³/mV]	1136 ±100	1876 ±136	1719±106

[DOI: 10.1299/jamdsm.2024jamdsm0018]
© 2024 The Japan Society of Mechanical Engineers

The optimised values of $\{b_{nom}, \alpha_L, g_{0,nom}, \sigma\}$ found in each case were then evaluated in a separate Monte-Carlo simulation with 256 random samples, where the dimensions vary from sample to sample according to the estimations from section 3.2. The results are summarised in Table 3. As expected, Case I resulted in a thin beam (even with the minimum allowed thickness), and the penalty function effectively led the evolutionary strategy to select the narrowest gap that would not correspond to a pull-in below 25 V—such a small gap, nonetheless, comes at the cost of a too low Q factor and a low overall sensitivity ($S_{tot} = N_{osc} H_0 f_{dyn}$). Consideration of the Q factor in Case II yielded a much larger gap, which resulted in a higher overall sensitivity (despite a much smaller static sensitivity, H_0) whose limit this time was the maximum allowed Q factor, not pull-in. Upon introduction of the SAA routine, the optimised dimensions in Case III were such that the natural frequency, even including the expected process variations, was better contained within the desired range of 20 ± 1 kHz. A small price was paid in the reduction of the overall sensitivity with respect to Case II, but the variance of all performance metrics was also consistently reduced. It is noteworthy that the shape factor for the electrostatic gap (σ) converged to nearly 1.0 in all three cases, showing that this curved geometry is advantageous for a higher sensitivity.

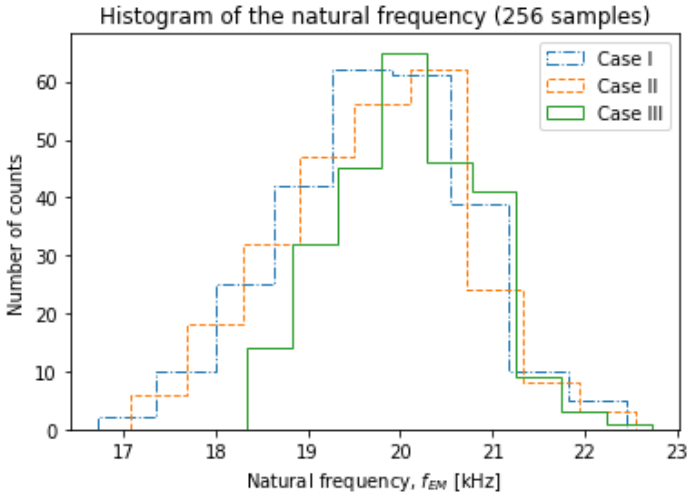

Fig. 6 Histogram of the natural frequency of the three optimisation cases, all undergoing the same random process variations according to the estimation in section 3.2.

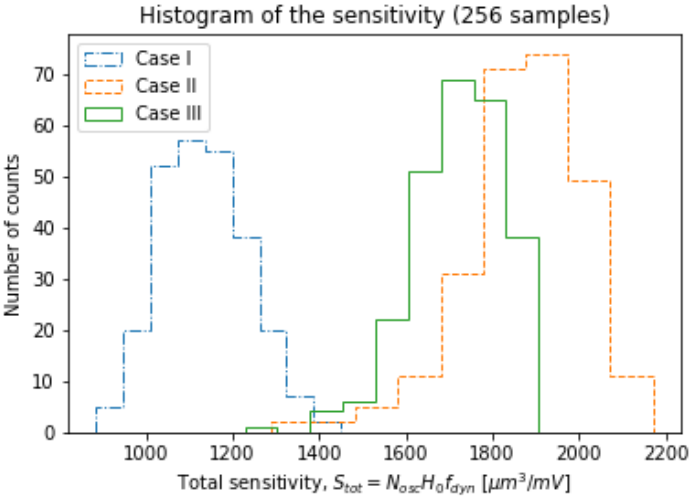

Fig. 7 Histogram of the total sensitivity of the three optimisation cases, all undergoing the same random process variations according to the estimation in section 3.2.

Figures 6 and 7 present histograms of the natural frequency and total sensitivity, respectively, for the three optimisation cases. The histogram in Fig. 6 shows how the optimised dimensions in Case III lead to a variation in the natural frequency that is mostly contained between 19 and 21 kHz, as desired, whereas in Case I and Case II there is a

[DOI: 10.1299/jamdsm.2024jamdsm0018]
© 2024 The Japan Society of Mechanical Engineers

higher number of samples whose natural frequency lies below 19 kHz. The impact of the different optimisation cases is better appreciated in Fig. 7. The sensitivity in Case I is the lowest of all three due to the neglect of the Q factor in the optimisation, whereas the sensitivity in Case II, which included this effect, is indeed the highest. As process variations are considered in the design through SAA (Case III), the average value of the sensitivity is slightly reduced, but its variance is also lowered.

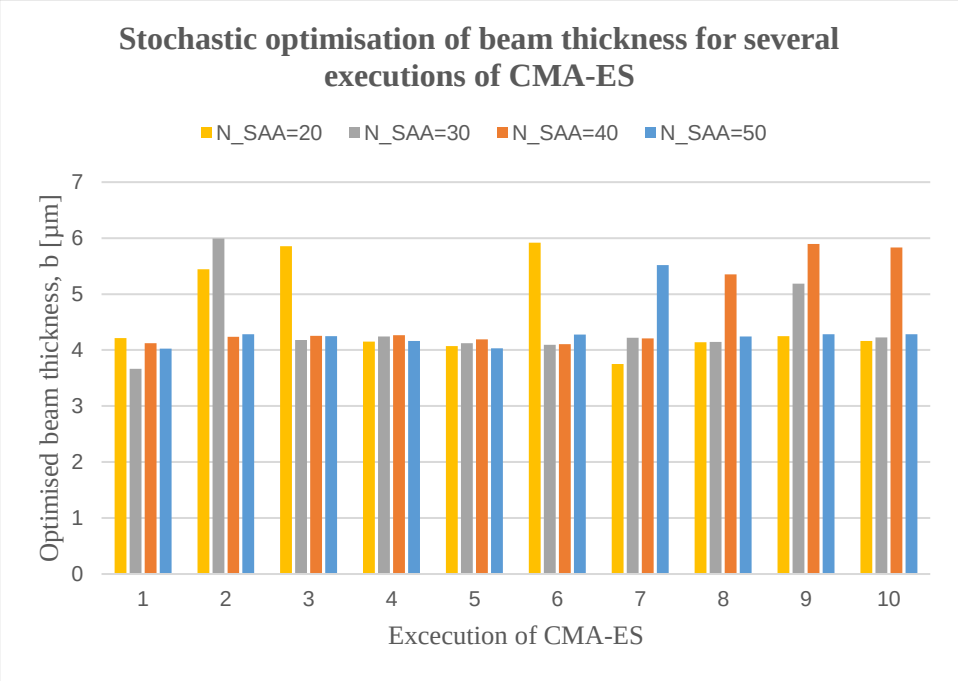

Fig. 8 Effect of the population size used for SAA (N_{SAA}) on the outcome of the optimisation routine, particularly the optimised beam thickness. Ten independent executions of CMA-ES are compared for four different population sizes, evidencing how approximately 50 random samples are required to stabilise the outcome of the optimisation.

A consequence of utilising SAA within CMA-ES is that there is a double randomness in the optimisation procedure: both in the evolutionary strategy and in the outcome of the objective function itself. Given that a random process has been introduced for the generation of a finite number of samples, the calculated average of the objective function (which serves as an approximation of the expected value) exhibits a certain random fluctuation, which can be reduced with a large enough population size. This begs the question as to whether CMA-ES converges towards a stable value under these conditions. Figure 8 presents the outcome of independent executions of the optimisation routine, comparing four different population sizes ranging from 20 to 50 samples. Although most of the executions do converge towards a beam thickness of ~ 4.2 µm, some executions did result in a significantly larger thickness near 6 µm. This is likely related to the fact that, in addition to the fluctuations of the objective function, a staircase function is involved in the calculation of the number of oscillators (N_{osc}), which has a potential to deviate CMA-ES towards a competing local maximum. As the number of samples is increased to 50, the likelihood of such a deviated outcome is effectively reduced.

5. Conclusions

The design of micromachines under the uncertainty of process variations can be formulated as a single-objective optimisation problem with simple bounds for the design parameters. This can be achieved by expressing the design target as the maximisation of an expected value, and approximating this expected value as the arithmetic mean of a finite number of samples that undergo the effect of random variations. This is known in stochastic programming as Sample-Average Approximation. Combined with a genetic algorithm, CMA-ES, the optimal parameters of a design under uncertainty can be found without requiring a computation of a gradient nor an analytic expression of the objective function. Additional conditions such as a safe operation (without static nor dynamic failure) and a tight tolerance in the resonance frequency—which impose implicit, nonlinear constraints on the search space—can be

[DOI: 10.1299/jamdsm.2024jamdsm0018]
© 2024 The Japan Society of Mechanical Engineers

effectively considered in this optimisation routine by means of penalty functions. This optimisation strategy was tested for the design case of an electrostatic ultrasonic transducer, which requires both the resonance frequency to lie within a specific range and the sensitivity to be maximised—without failure due to pull-in taking place. This design case is suitable, since analytic expressions are available to predict its sensitivity, resonance frequency, pull-in and number of oscillators in a given chip area, but if such models are not available, this design strategy can also be performed with a finite-element simulation. Optical measurements of an existing design were used to estimate the expected random process variations in a hypothetical design. Comparison of optimisation outcomes with and without the Sample-Average Approximation shows how an a priori estimation of process variations leads to a more conservative choice of the design parameters in order to uphold the constraints even under variable dimensions.

Acknowledgement

This work was supported by the Fraunhofer Internal Programmes under Grant No. SME 685 400.

References

Bao, M. and Yang, H., Squeeze-film air damping in MEMS, Sensors and Actuators A: Physical, Vol. 136, No. 1 (2007), DOI: 10.1016/j.sna.2007.01.008.

Beranek, L. L., Acoustics (1993), pp. 91-108, Acoustical Society of America.

Colette, Y., Hansen, N., Pujol, G., Salazar Aponte, D. and Le Riche, R., Object-oriented programming of optimizers — examples in Scilab, in Breitkopf, P. and Coelho, R. J. (eds.), Multidisciplinary Design Optimization in Computational Mechanics (2013), pp. 499-538, Wiley, DOI: 10.1002/9781118600153.ch14.

Díaz, J. O., A feature-to-wafer-scale model of etch-rate non-uniformity in deep reactive ion etching, M. S. Thesis, Massachusetts Institute of Technology (2010).

Dornfeld, D. A. and Lee, D.-E., Precision Manufacturing (2010), pp. 1-7, Springer-Verlag.

Fan, Z., Wang, J. and Goodman, E., An evolutionary approach for robust layout synthesis of MEMS, Proceedings of the 2005 IEEE/ASME International Conference on Advanced Intelligent Mechatronics (2005), pp. 1186-1191, DOI: 10.1109/AIM.2005.1511171.

Hansen, N. and Ostermeier, A., Adapting arbitrary normal mutation distributions in evolution strategies: the co-variance matrix adaptation, Proceedings of IEEE International Conference on Evolutionary Computation (1996), pp. 312-317, DOI: 10.1109/ICEC.1996.542381.

Hsiung, K.-L., Design of microelectromechanical systems for variability via chance-constrained optimization, Journal of Physics: Conference Series, Vol. 34, No. 162 (2006), pp. 162-167, DOI 10.1088/1742-6596/34/1/027.

Kim, S., Pasupathy, R. and Henderson, S., A guide to sample-average approximation, in Fu, M. C. (eds.), Handbook of Simulation Optimization (2015), pp. 207-243, Springer New York, DOI: 10.1007/978-1-4939-1384-8_8.

Mawardi, A. and Pitchumani, R., Design of microresonators under uncertainty, Journal of Microelectromechanical Systems, Vol. 14, No. 1 (2005), pp. 63-69, DOI: 10.1109/JMEMS.2004.839021.

Monsalve, J. M., Melnikov, A., Stolz, M., Mrosk, A., Jongmanns, M., Wall, F., Langa, S., Marica-Bercu, I., Brändel, T., Kircher, M., Schenk, H. A. G., Kaiser, B. and Schenk, H., Proof of concept of an air-coupled electrostatic ultrasonic transducer based on lateral motion, Sensors and Actuators A: Physical, Vol. 345 (2022), Paper No. 113813, DOI: 10.1016/j.sna.2022.113813.

Monsalve, J. M., Kaiser, B. and Schenk, H., Design of micromachined electrostatic transducers for variability with the sample-average approximation method, Proceedings of the MikroSystemTechnik Congress 2023 (2023), Paper No. 639.

Nagata, Y., The lens design using the CMA-ES algorithm, in: Deb, K. (eds.) Genetic and Evolutionary Computation – GECCO 2004, Vol. 3103 (2004), pp. 1189-1200, Springer, Berlin, Heidelberg, DOI: 10.1007/978-3-540-24855-2_127.

Safaie, B. K., Shamshirsaz, M. and Bahrami, M., Robust design under uncertainties of electro-thermal microactuator, Proceedings of the 2014 Symposium on Design, Test, Integration and Packaging of MEMS/MOEMS (DTIP) (2014), pp. 1-6, DOI: 10.1109/DTIP.2014.7056698.

Saghir, S., Saleem, M. M., Hamza, A., Riaz, K., Iqbal, S. and Shakoor, R. I., A Systematic design optimization

 © 2024 The Japan Society of Mechanical Engineers

approach for multiphysics MEMS devices based on combined computer experiments and Gaussian process modeling, Sensors, Vol. 21 (2021), Paper No. 7242, DOI: 10.3390/s21217242.

Schenk, H. A. G., Melnikov, A., Wall, F., Gaudet, M. and Stolz, M., Electrically actuated microbeams: an explicit calculation of the Coulomb integral in the entire stable and unstable regimes using a Chebyshev-Edgeworth approach, Physical Review Applied, Vol. 18, No. 1 (2022), DOI: 10.1103/PhysRevApplied.18.014059.

Schuffenhauer, D., Numerical optimisation of microactuators, M. S. Thesis, Brandenburg University of Cottbus (2017) (in German).

Sharpe, W. N., Jackson, K. M., Hemker, K. J. and Xie, Z., Effect of specimen size on Young's modulus and fracture strength of polysilicon, Journal of Microelectromechanical Systems, Vol. 10, No. 3 (2001), pp. 317-326, DOI: 10.1109/84.946774.

Wall, F., Schenk, H. A. G., Melnikov, A. and Monsalve, J. M., Squeeze film damping by a structured cavity in an air-coupled electrostatic ultrasonic transducer, Proceedings of the 29th International Congress on Sound and Vibration ICSV29 (2023), Paper No. 210.

Wang, Y., Pan, B., Tu, W., Liu, P., Jiang, B., Gao, C., Lu, W., Jui, S., Kong, L., Sample average approximation for stochastic optimization with dependent data: performance guarantees and tractability, Proceedings of the AAAI Conference on Artificial Intelligence, Vol. 36, No. 4 (2022), DOI: 10.1609/aaai.v36i4.20301.

[DOI: 10.1299/jamdsm.2024jamdsm0018]
© 2024 The Japan Society of Mechanical Engineers